2001, Quantitative Approaches in Systems Analysis, 23, 43-54.
Special issue "Forum of Methodology: The C.T. de Wit Graduate Schoolfor Production Ecology & Resource Conservation" (A. Stein, T.H. Jetten and A.G.T. Schut, eds.)

Image analysis in agricultural research

C.A. Glasbey and G.W. Horgan
Biomathematics and Statistics Scotland
JCMB, King's Buildings, Edinburgh, EH9 3JZ, Scotland

Abstract

We give an overview of image analysis, particularly as it relates to agricultural and environmental research. In turn we consider three stages of analysis: image enhancement, segmentation and taking measurements. Enhancement is a set of methods for modifying images to reduce the effects of noise, blurring and warping/distortion of the image frame. Segmentation is the process of sub-dividing an image into regions, which correspond to different objects or parts of objects. Finally, extraction of quantitative information is the end-point of most image analysis in agricultural research. The aim may simply be to count the number of objects in a scene, or measure their areas, or it may be more complex, such as describing the shapes of objects in order to discriminate between them. We illustrate these three stages of analysis using a diverse set of images, ranging from DNA microarrays to aerial photographs.

1 Introduction

The extraction of information from images is a task that we humans do most of our waking lives; usually with little apparent effort. It is what you are doing in reading these words! The term 'image analysis' has come to mean the use of computers to interpret digital versions of images. Such methods are of increasing relevance in all sciences, including agricultural and environmental research. For example, Fig 1(a) shows a colour image of a DNA microarray approximately 2 cm square. Microarrays are a powerful new set of genomic methods for monitoring the expression of thousands of genes simultaneously (see, for example, Chipping Forecast, 1999). For differential gene expression, the genes are placed as spots on a glass slide, which is then hybridized with two samples, each labelled with a fluorescent marker, and the microarray is scanned at the two wavelengths. In Fig 1(a), red spots reveal genes only expressed by virus one, green spots show genes only expressed by virus two, yellow spots show genes expressed by both viruses and dark spots by neither. At a totally different physical scale, Fig 1(c) shows a section of an aerial black-and-white photograph, about $\frac{1}{2}$km $\times$ $\frac{1}{2}$km at 1m resolution, of an area of heather moorland in Glen Feshie, Scotland. The lighter patches are areas of muirburn, a type of land management in which heather is burnt in order to encourage growth of young vigorous heather, a habitat particularly suitable for red grouse. Such photographs are an efficient means of mapping changes over time in land use and the distribution of semi-natural vegetation. Finally, Figs 1(b) and (d) show colour photographs of samples of pea pods and leaflets, from which horticultural scientists wish to extract measurements of size and shape in order to discriminate between varieties.

The human vision system is a 'hard act to follow', but computers offer the possibility to relieve scientists of much tedious work in extracting quantitative information, and can sometimes transform images in ways that were not previously possible. Digital image analysis is a broad, interdisciplinary field with many challenging problems to which statistical methods are applicable (see, for example, Serra, 1982; Jain, 1989; Glasbey and Horgan, 1995). An image usually consists of a rectangular array of pixels, each of which measures the brightness of a part of the original scene, where 'brightness' may denote reflected light but could equally represent any other variate that has been measured on a 2D grid. Methods of analysis range from low-level processing of individual pixels or small neighbourhoods, such as the use of filters to enhance images, through segmentation, the spatial clustering of pixels into segments that represent regions or objects, to high-level processing, where the information in whole images is summarised. We will consider each of these stages in turn, using images in Fig 1 for illustration.

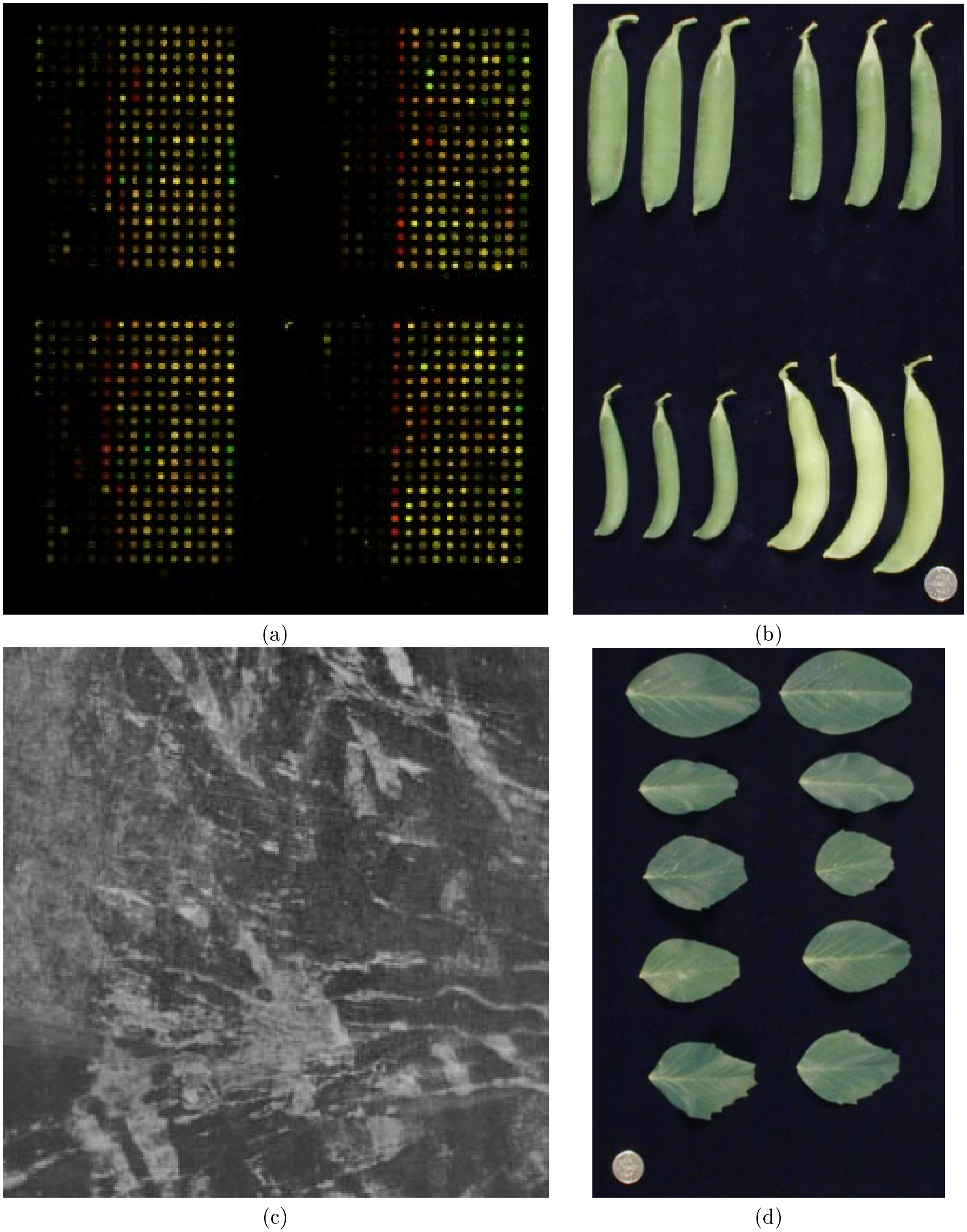

Figure 1: Illustrative images: **(a)** a DNA microarray, **(b)** a colour photograph of pea pods (with a coin included to enable scale calibration), **(c)** an aerial photograph of Glen Feshie, Scotland, **(d)** a colour photograph of pea leaflets.

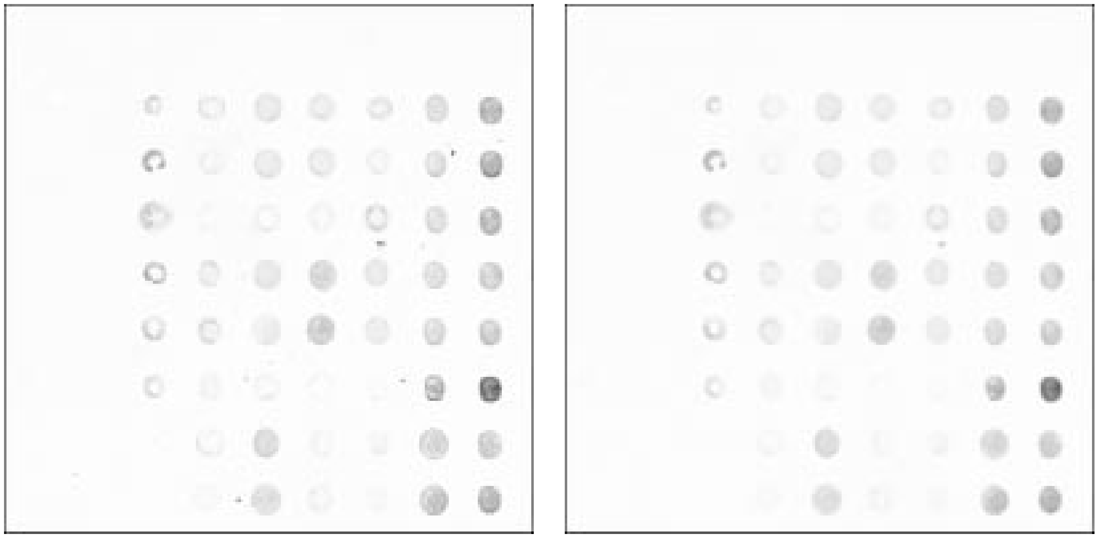

(a) (b)

Figure 2: Enlargement of red colour band for top-left corner of Fig 1(a): **(a)** original, with reversed grey-scale, **(b)** after applying a 5 × 5 median filter.

2 Enhancement

All images are subject to some degradation from their ideal forms, whether this is the presence of noise, blurring, or a distortion of the image frame. Image enhancement is a set of methods for modifying images to reduce these effects, both to aid human interpretation and as a precursor to further analysis. In turn, we will consider filters, unwarping and interpolation.

Filters have two roles in image analysis, either to reduce noise by smoothing or to emphasise edges, i.e., boundaries between objects or parts of objects. Filters are linear if the output values are linear combinations of the pixels in the original image, otherwise they are nonlinear. Linear filters are well understood and fast to compute. They can be studied and implemented in either spatial or frequency domains. Linear filters can be categorised as low-pass or high-pass, according to whether they smooth by removing high frequency components in images, or emphasise edges by removing low frequency components. A third category, band-pass filters, remove both the lowest and highest frequencies from images. Use of the Fast Fourier Transform leads to efficient computation for filters larger than 5 × 5. Further details can be found in Glasbey and Horgan (1995, chapter 3). Note that smoothing filters are a form of kernel regression. See, for example, Hastie and Tibshirani (1990, chapter 2) for a review of this and alternative statistical approaches to smoothing.

In filtering to reduce noise levels, linear smoothing filters inevitably blur edges, because both edges and noise are high-frequency components of images. Nonlinear filters are able to simultaneously reduce noise and preserve edges, but they have less secure theoretical foundations and can be slow to compute. The simplest, most studied and most widely used nonlinear filter is the moving median. However, many other robust estimators of location have also been used (Fong et al., 1989). Multiresolution methods based on wavelets are a new approach to smoothing images (Donoho et al., 1995), which also offer great potential in other areas of image analysis. Fig 2 illustrates the application of a median filter to one of the colour bands in Fig 1(a). For a filter of size $(2m+1) \times (2m+1)$ the output is

$$z_{i,j} = \text{ median } \{y_{i+k,j+l} \ : \ k,l = -m,\ldots,m\}$$

where $y_{i,j}$ denotes the original pixel value in row i, column j. We see, in Fig 2(b), that most of the speckle noise has been removed.

Many nonlinear filters are designed to be spatially adaptive – that is, the filtering operation carried out is dependent on some feature of the neighbourhood of a pixel. For example, Tomita and Tsuji (1977) proposed a variance-based filter. They obtained the mean and variance in five

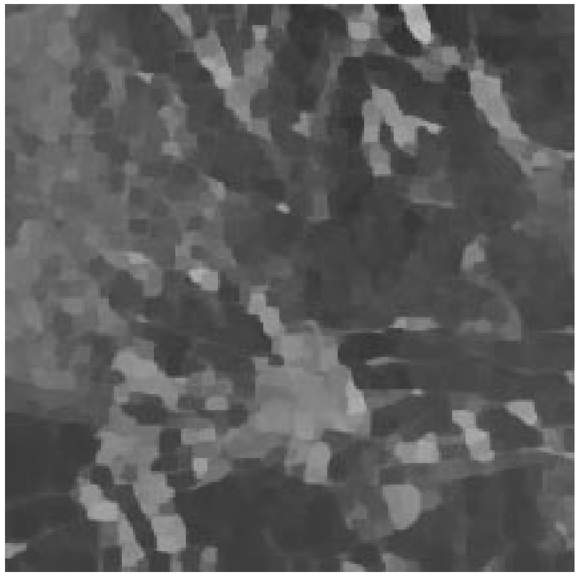

Figure 3: Aerial photo image in Fig 1(c) smoothed by spatially adaptive filter which selects mean of whichever 7×7 window containing the pixel has minimum variance.

$(2m+1) \times (2m+1)$ windows, which placed the pixel being filtered at the four corners or the centre, and defined the filter output to be the mean of that window which had the smallest variance. This filter is based on the idea that each pixel belongs to one of a number of internally homogeneous regions, and that one of the five windows (and perhaps only one for a pixel near a region boundary) will lie completely or mainly within the region to which the pixel belongs. That window should have minimum variance, and its mean is then an estimate of the mean intensity for the region. The filter is readily extended to more than five windows. Fig 3 shows the results of applying this filter to Fig 1(c), using *all* 7×7 windows containing the pixel being filtered.

For descriptions of yet more filters, and comparative studies of performance, the interested reader is referred to the review papers of Chin and Yeh (1983); Wang et al. (1983); Mastin (1985); Fong et al. (1989); Imme (1991); Wu et al. (1992). Unfortunately, the reviews are ultimately inconclusive and contradictory, because images can be of such varying types and there is no unique measure of a filter's success.

Morphological filters are a subclass of nonlinear filters, but also the building blocks for a theory of image analysis (Serra, 1982, 1988). The simplest filters are based on 'max' and 'min' operations. Substantial improvements in images can often be achieved using sequences of such filters. For example, another problem with Fig 1(a) is that the brightness in the background varies. This is a common problem in image analysis, and makes comparison of similar features in different parts of an image difficult. A 'morphological closing' of the image can be used to estimate the background trend. The simplest closings are obtained by first replacing each pixel by the maximum local intensity in a region (for example, using a structuring element which is a disc of radius R centered on each pixel), and then performing a similar operation on the resulting image, using the local minimum. Mathematically, the pixels, z_{ij}, in the closed image will be given by

$$z_{ij} = \min_{k,l} \; x_{i+k,j+l} \quad \text{where } x_{ij} = \max_{k,l} \; y_{i+k,j+l}, \quad \text{for } (k^2+l^2)^{1/2} \leq R$$

with $y_{i,j}$ again denoting the original pixel values. If this filter is applied to Fig 4(a), then only the small groups of pixels which are darker than their surroundings will be substantially changed from y_{ij} to z_{ij}. These are the spots. By subtracting z from y, these spots will be made more distinct. Fig 4(c) shows the result using a disc of radius 21 pixels. This is known as a 'top-hat filter', and was proposed in this application by Yang et al. (2000).

Unwarping of images is an important stage in many applications of image analysis (Glasbey and Mardia, 1998, 2001). It may be needed to remove optical distortions introduced by a camera or viewing perspective (Tang and Suen, 1993), to register an image with a reference grid such as a map,

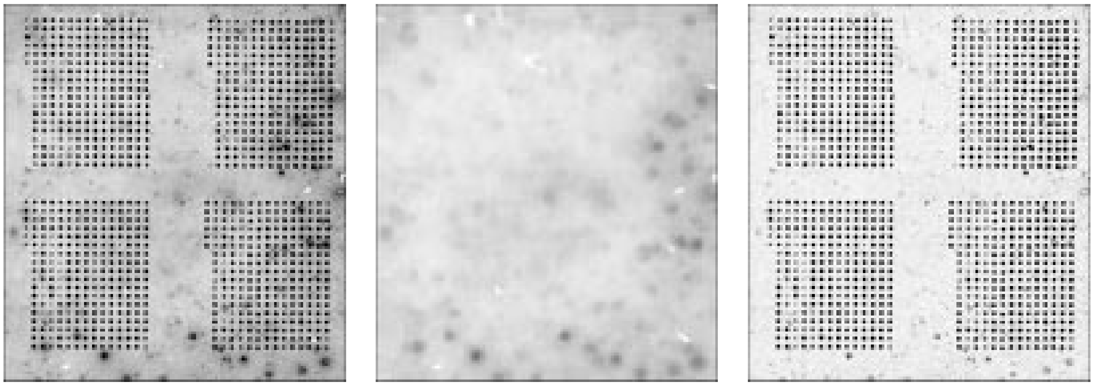

(a) (b) (c)

Figure 4: Application of trend removal to red colour band in Fig 1(a), after median filtering: **(a)** original, with reversed and stretched grey-scale, **(b)** trend estimated by morphological closing, **(c)** after subtraction of trend.

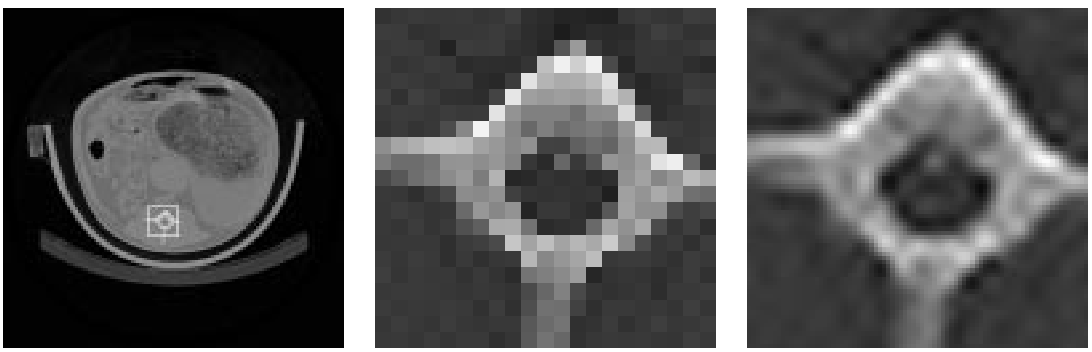

(a) (b) (c)

Figure 5: X-ray CT lumbar image of a sheep: **(a)** full image (256×256), **(b)** magnified sub-image of backbone identified by white square in (a), **(c)** quarter-pixel interpolation of (b).

or to align two or more images (Brown, 1992). For example, matching is important in reconstructing three-dimensional shape from either a series of two-dimensional sections or stereoscopic pairs of images. Much effort has been expended in developing algorithms for registering satellite images with both geographic information systems and with other forms of remote sensing system, such as optical sensors and synthetic aperture radar (see, for example, Richards, 1986, chapter 2). Recently there has been considerable interest in registering images produced by medical sensing systems with body atlas information (Colchester and Hawkes, 1991, §3). Combined images produced using different imaging modalities also have great potential. For example, X-ray images reveal structure, whereas magnetic resonance images reveal functionality, so their synthesis generates more informative images.

Although digital images typically consist of pixel values at nodes of a square lattice, interpolated values at other locations are needed for many reasons, including image enlargement to aid visual inspection, and warping to register with another frame of reference. In particular, such problems occur frequently with medical images, where it is not usually possible to enlarge an image by increasing the resolution of the imaging sensor. To illustrate, Fig 5(a) shows an X-ray computed tomography (CT) image of the lumbar region of a sheep, and Fig 5(b) shows an enlargement of the backbone, visual interpretation of which is hindered by the pixellation. Fig 5(c) shows the results of interpolating Fig 5(b) to quarter-pixel resolution, using a method based on optimal linear interpolation in the frequency domain (Glasbey, 2001).

3 Segmentation

Segmentation is the term given in the image processing literature to the process of sub-dividing an image into regions, which correspond to different objects or parts of objects. Every pixel is allocated to one of a number of regions or categories. A good segmentation is typically one in which pixels which have been placed in the same category have similar values and form a connected region, and are dissimilar to neighbouring pixels which have been placed in other categories. Segmentation is often the critical step in image analysis: the point at which we move from considering each pixel as a unit of observation to working with objects (or parts of objects) in the image, composed of many pixels. It is needed before measurements can be made on images, such as intensities of spots in DNA microarrays, or areas of land in an aerial photograph. If the segmentation is done well then all other stages in image analysis are made simpler. However, success is often only partial.

There are four generic approaches to segmentation: thresholding, edge-, region- and model-based (for a review, see Haralick and Shapiro, 1992). In thresholding, pixels are allocated to categories according to the range of values in which a pixel lies. In edge-based segmentation, an edge filter is applied to the image, pixels are classified as edge or non-edge depending on the filter output, and pixels which are not separated by an edge are allocated to the same category. Region-based segmentation algorithms operate iteratively by grouping together pixels which are neighbours and have similar values, and splitting groups of pixels which are dissimilar in value. Finally, model-based methods include the use of Bayesian inference and stochastic templates (Grenander, 1996).

Edge-based methods are straightforward in principle, and there is a huge range of edge detection algorithms available. Where they encounter difficulty is in that most edge finding methods do not produce continuous closed curves, which the boundary of a region must be. Effort must then be expended in overcoming this, either by trying to join up the edges, or in some other way. Region based methods do not suffer these difficulties, and many variations on this idea have also been proposed. One feature of these methods is that they tend to produce results which are not isotropic (independent of direction) and depend on whether the algorithm passes through the image from top to bottom, left to right or vice versa.

Fig 6(a) shows the result of a region based segmentation of the aerial photo, Fig 1(c). This is based on a variation of the spatial clustering algorithm proposed by Haralick and Shapiro (1992). The algorithm passes from left to right and top to bottom (an arbitrary choice) of the smoothed image, Fig 3, creating clusters. A pixel is added to a cluster adjacent to it if its intensity differs from the mean intensity of the cluster by less than some threshold a_1. Otherwise a new cluster is created. A reverse sweep is then made through the image joining adjacent clusters if their mean intensities differ by less than another threshold a_2. Results will be affected by the choice of a_1 and a_2, and there is little other than trial-and-error to guide their choice. Directional artifacts are not apparent, however. It is only by defining a model for the image that a segmentation method can be developed with some objective approach to parameter selection.

The areas and mean intensities of segments can be used to further segment Fig 6(a) in order to find areas of muirburn. These are the brighter areas in the image, and by identifying regions which had mean intensity greater than I_M, and area A satisfying $A_1 \leq A \leq A_2$, regions of muirburn are effectively isolated, as shown in Fig 6(b), with the segment boundaries superimposed on the original image. The area condition is based on knowledge that muirburn, a result of land management, does not occur over either very small or very large patches of land.

As an example of a model-based method, Young et al. (1998) developed a method for constructing templates of cells in differential interference contrast (DIC) microscopy, taking into account DIC optics. Fig 7(a) shows the template for a cell at a particular orientation, and Fig 7(b) shows the result of automatically segmenting an image containing several *Candida* yeast cells.

Although fully-automatic image analysis is the ideal, semi-automatic methods are often the reality: a human-computer symbiosis. Consider boundary detection: a person can accurately locate objects in noisy images and roughly outline them, whereas computers provide smooth, accurate and detailed outlines much more quickly, but fail occasionally. Human and computer inputs can be combined by the computer refining a user-supplied outline to optimise a smoothness and edge-following criterion, or by the user modifying computer-generated boundaries. Most published research has focused on fully-automatic algorithms, even though semi-automatic methods are often more practicable: they

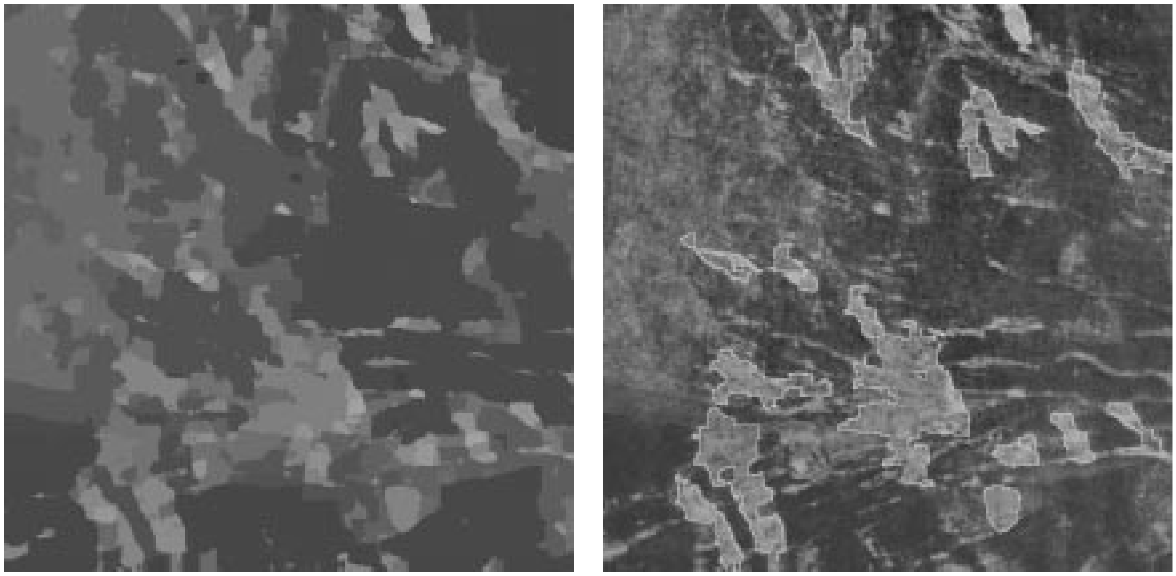

(a) (b)

Figure 6: *Segmentation of aerial photo image in Fig 1(c):* **(a)** *result of applying spatial clustering algorithm to Fig 3,* **(b)** *automatic detection of muirburn, by applying decision rule to (a).*

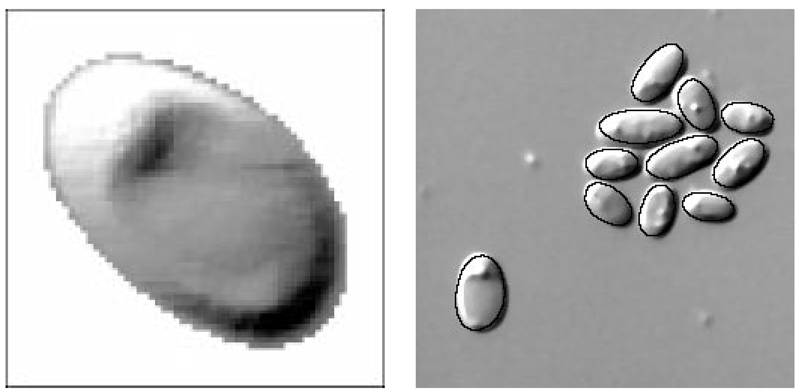

Figure 7: *Candida* yeast cells: **(a)** example of template for cell at orientation of 45°. **(b)** DIC microscope image with identified cell boundaries superimposed.

avoid the need for an algorithm to be very precise or much effort to be expended to automate what people can do easily, if laboriously, by eye. Samadani and Han (1993) distinguished two types of semi-automatic algorithm: batch methods, where inputs from a user are subsequently refined by the computer, and interactive methods, which combine simultaneous user and computer inputs. Also, the nature and intensity of user input is important, and can take many forms. It may simply involve locating a few points on a boundary, between which the algorithm interpolates (Wu and Barba, 1995). Alternatively, a complete boundary may need to be input, or user intervention may just be an option within a system, to be used if and when necessary. For interactive computer systems, see Frey (1969); Ramesh et al. (1992); Ruiz and Fairhurst (1995).

4 Measurement

The extraction of quantitative information is the end-point of most image analysis in agricultural research. The aim may simply be to count the number of objects in a scene, or measure their areas, or it may be more complex, such as describing the shapes of objects in order to discriminate between

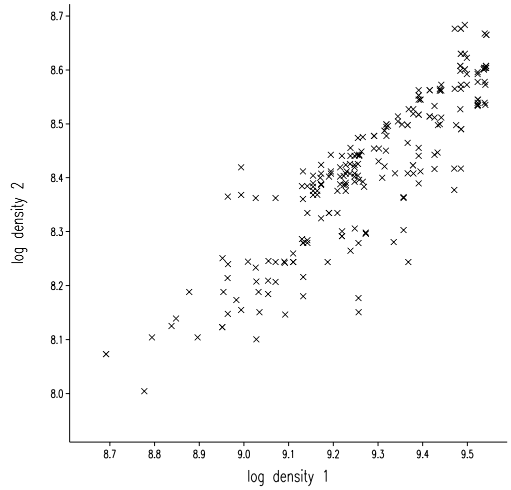

Figure 8: Plot of pixel values in top-right spot in Fig 2(b).

them.

It is a straightforward matter to count the number of objects in an image provided that the segmentation has successfully associated one, and only one, component with each object. If this is not the case, then manual intervention may be necessary to complete the segmentation. However, short-cuts can sometimes be taken. For example, if the mean size of objects is known, then the number of objects in an image can be estimated even when they are touching, through dividing the total area covered by all the objects by this average size. It is even possible to make allowance for objects overlapping each other provided that this process can be modeled, for instance by assuming that objects are positioned at random over the image and making use of the properties of Boolean models (Cressie, 1991, pp 753-759). For example, Jeulin (1993) has estimated the size distribution of a powder in such a way.

For the DNA microarray in Fig 1(a), we wish to estimate the difference in spot intensity between the red and green colour bands. Fig 8 shows a scatter plot of the log-transformed pixel values for a single spot, from which the assumption of a bivariate log-normal distribution looks reasonable. (For alternative approaches, see Chen et al., 1997; Newton et al., 2001). Therefore, the maximum likelihood estimator of the differential rate of expression, given by

$$\exp\left[\frac{1}{n}\sum_{i,j}\log\left(y_{i,j}^{(2)}/y_{i,j}^{(1)}\right)\right],$$

where n denotes the number of pixels in the spot, will be more efficient than the standard method of forming the ratio of means:

$$\frac{\sum_{i,j} y_{i,j}^{(2)}}{\sum_{i,j} y_{i,j}^{(1)}}.$$

However, simulations show the difference in efficiency to be small.

Very many measures of shape can be defined, depending on the features considered relevant. For example, in Figs 1(b) and (d) there is very little difficulty in segmentation into individual pods or leaves and background. Size is then readily measured from the area of each object. Some other measurements are illustrated in Figs 9. Width can be measured from the diameter of the maximum disk which fits inside an object, a morphological measurement. For the pods, length is measured as the boundary along the longer edge of each pod, and the curvature is measured as the ratio of this length to the length measured directly from top to bottom. This raises the issue of orientation. For measuring the length, we wish to have the pods or leaflets in a fixed orientation. We can do this by defining the orientation as that of the major (or principal) axis of the object. This, and the minor

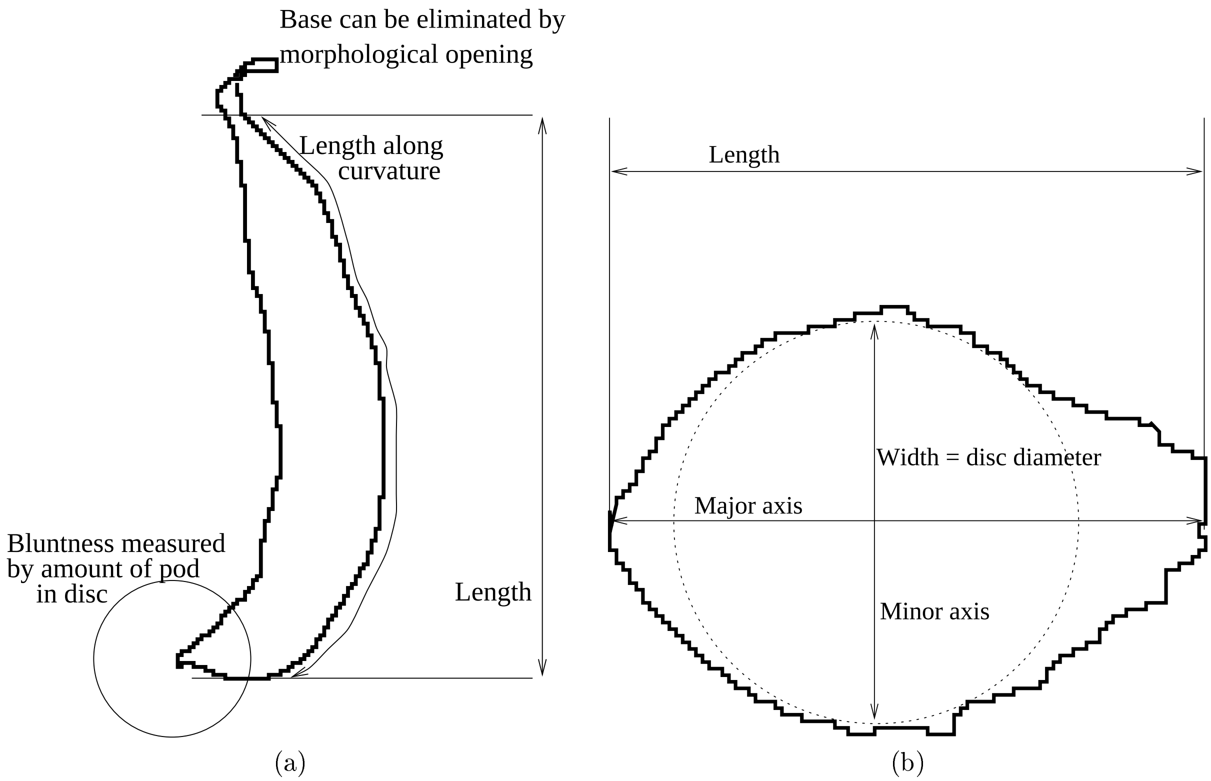

Figure 9: Illustration of size measurements: **(a)** for pea pods, **(b)** for pea leaflets.

axis which is perpendicular to it, can be obtained from the second moments in the horizontal and vertical directions (the $(k,l)^{th}$ moment of an object being defined as the sum, over pixel positions (i,j) in the object, of $(i-\bar{i})^k(j-\bar{j})^l$). The ratio of the moments in the direction of the major and minor axes measures the elongation of the object. Compactness, defined as the ratio of the square of the perimeter to the area, is a related measure which is also minimised for a disc, but it is also sensitive to how rough the boundary is. This is a relevant measure for the pea leaflets. Other definitions of this property can be obtained from the autocorrelation of the boundary direction as the outline is traced. Shape can be measured for particular features of an object. For example, the bluntness of the tip of a pod is considered relevant. This can be defined as the proportion of a disc, of some specified radius, centred on the tip which is occupied by the pod. For other examples of the use of such shape measures in horticultural applications, see Bleasdale and Thompson (1963); Keefe and Draper (1988); van de Vooren and van der Heijden (1993); van der Heijden et al. (1996).

Perimeters of objects are useful summary statistics. Let P denote the number of pixels on the boundary of object A, specified as follows. Pixel (i,j) is on the boundary if $(i,j) \in A$, but one of its four horizontal or vertical neighbours is outside the object, i.e.,

$$(i+1,j) \notin A \quad \text{or } (i-1,j) \notin A \quad \text{or } (i,j+1) \notin A \quad \text{or } (i,j-1) \notin A.$$

This gives an 8-connected boundary, with pixels linked either horizontally, vertically or diagonally. An unbiased estimator of the perimeter is given by

$$\frac{4}{\pi}\frac{P}{\sqrt{2}}$$

provided that either all orientations in the boundary occur equally often or the sampling grid is positioned randomly on the object. This, and more complicated methods for estimating perimeters, are considered by Koplowitz and Bruckstein (1989). The use of scaling factors is part of stereology, a field which has traditionally been concerned with inference about objects using information from lower-dimensional samples — such as estimating volumes of objects from the areas of intersection with randomly positioned cutting planes (see, for example, Stoyan et al., 1995, chapter 11). In particular, the scaling factor of $\pi/4$ arises in two of the so-called ‘six fundamental formulae’ of classical stereology. Note further, that mathematical morphology can be used to study size distributions of objects in images. By performing openings, using structuring elements at a range of different sizes, a granulometry can be obtained (Serra, 1982, chapter 10).

Shape information is what remains once location, orientation and size features of an object have been dealt with. Its description is an open-ended task, because there are potentially so many aspects to an object even after location, orientation and size effects have been removed. Approaches other than those already discussed, include the use of landmarks (Dryden and Mardia, 1998) and warpings such as thin-plate splines and other morphometric methods (Bookstein, 1991), which consider image plane distortions needed to move landmarks to designated locations. Rohlf and Archie (1984) and Mou and Stoermer (1992) compared alternative forms of Fourier descriptors to approximate object boundaries, and applied Zahn and Roskies (1972) method to describe the outlines respectively of mosquito wings and diatoms.

5 Discussion

It seems likely that image analysis techniques will continue to grow in power and utility, and the achievements of human vision will gradually be replicated by computers. At the same time, we hope to see a convergence in the disparate approaches to image analysis, and the emergence of a more systematic approach to replace much of the present empiricism.

There are great opportunities for image quantification and comparison beyond the capabilities of human vision. For example, large databases of medical images currently being accumulated could be used to estimate the normal ranges of organ sizes and shapes, against which to judge new samples. Similarly, the vast archives of remotely-sensed images could be put to much greater use than currently. Further, new technologies will yield different types of images, for which new methodologies will be required. Also, there is increasing interest in integrating information from different imaging modalities, for example, MRI, which provides soft tissue detail, and X-ray CT, which provides bone detail.

Acknowledgements

The work reported here was supported by funds from the Scottish Executive Rural Affairs Department. We are grateful to The Scottish Centre for Genome Technology and Informatics, Scottish Agricultural Science Agency and Macaulay Land Use Research Institute for permission to use the images.

References

Bleasdale, J. K. A. and Thompson, R. (1963). An objective method of recording and comparing the shapes of carrot roots. *Journal of Horticultural Science*, 38:232–241.

Bookstein, F. L. (1991). *Morphometric Tools for Landmark Data*. Cambridge University Press, Cambridge.

Brown, L. G. (1992). A survey of image registration techniques. *ACM Computing Surveys*, 24:325–376.

Chen, Y., Dougherty, E. R., and Bittner, M. L. (1997). Ratio based decisions and the quantitative analysis of cDNA microarray images. *Journal of Biomedical Optics*, 2:364–374.

Chin, R. T. and Yeh, C. (1983). Quantitative evaluation of some edge-preserving noise-smoothing techniques. *Computer Vision, Graphics and Image Processing*, 23:67–91.

Chipping Forecast (1999). *The Chipping Forecast*, volume 21 of *Supplement to Nature Genetics*.

Colchester, A. C. F. and Hawkes, D. J., editors (1991). *Information Processing in Medical Imaging. Proceeding of the 12th International Conference on Information Processing in Medical Imaging.* Springer-Verlag, Berlin.

Cressie, N. A. C. (1991). *Statistics for Spatial Data.* Wiley, New York.

Donoho, D. L., Johnstone, I. M., Kerkyacharian, G., and Picard, D. (1995). Wavelet shrinkage: asymptopia? (with discussion). *Journal of the Royal Statistical Society, Series B*, 57:301–369.

Dryden, I. L. and Mardia, K. V. (1998). *Statistical Shape Analysis.* Wiley, Chichester.

Fong, Y., Pomalaza-Raez, C. A., and Wang, X. (1989). Comparison study of nonlinear filters in image processing applications. *Optical Engineering*, 28:749–760.

Frey, H. S. (1969). An interactive computer program for chromosome analysis. *Computers and Biochemical Research*, 2:274–290.

Glasbey, C. A. (2001). Optimal linear interpolation of images with known point spread function. In *Scandinavian Image Analysis Conference – SCIA-2001.* (In press).

Glasbey, C. A. and Horgan, G. W. (1995). *Image Analysis for the Biological Sciences.* Wiley, Chichester.

Glasbey, C. A. and Mardia, K. V. (1998). A review of image warping methods. *Journal of Applied Statistics*, 25:155–171.

Glasbey, C. A. and Mardia, K. V. (2001). A penalised likelihood approach to image warping (with discussion). *Journal of the Royal Statistical Society, Series B*, 63. (In press).

Grenander, U. (1996). *Elements of Pattern Theory.* Johns Hopkins University Press, Baltimore.

Haralick, R. M. and Shapiro, L. G. (1992). *Computer and Robot Vision*, volume 1. Addison-Wesley, Reading, Massachusetts.

Hastie, T. J. and Tibshirani, R. J. (1990). *Generalized Additive Models.* Chapman and Hall, London.

Imme, M. (1991). A noise peak elimination filter. *CVGIP: Graphical Models and Image Processing*, 53:204–211.

Jain, A. K. (1989). *Fundamentals of Digital Image Processing.* Prentice-Hall International, New Jersey.

Jeulin, D. (1993). Random models for morphological analysis of powders. *Journal of Microscopy*, 172:13–21.

Keefe, P. D. and Draper, S. (1988). An automated machine vision system for the morphometry of new cultivars and plant genebank accessions. *Plant Varieties and Seeds*, 1:1–11.

Koplowitz, J. and Bruckstein, A. M. (1989). Design of perimeter estimators for digitized planar shapes. *IEEE Transactions on Pattern Analysis and Machine Intelligence*, 11:611–622.

Mastin, G. A. (1985). Adaptive filters for digital image noise smoothing: an evaluation. *Computer Vision, Graphics and Image Processing*, 31:103–121.

Mou, D. and Stoermer, E. F. (1992). Separating *Tabellaria* (Bacillariophyceae) shape groups based on Fourier descriptors. *Journal of Phycology*, 28:386–395.

Newton, M. A., Kenziorski, C. M., Richmond, C. S., Blattner, F. R., and Tsui, K. W. (2001). On differential variability of expression ratios: Improving statistical inference about gene expression changes from microarray data. *Journal of Computational Biology.* (In press).

Ramesh, B. V., Padaki, V. C., Hegde, K. S., Hazarika, D., and Verghese, C. A. (1992). An interactive image analysis system for quantitative cytology and to classify cervical cells. *Indian Journal of Medical Research*, 96:338–343.

Richards, J. A. (1986). *Remote Sensing Digital Image Analysis: An Introduction.* Springer-Verlag, Berlin.

Rohlf, F. J. and Archie, J. W. (1984). A comparison of Fourier methods for the description of wing shape in mosquitoes. *Systematic Zoology*, 33:302–317.

Ruiz, E. E. S. and Fairhurst, M. C. (1995). Improved approach to boundary location in 2-dimensional echocardiographic images. *IEE Proceedings, Vision, Image and Signal Processing*, 142:121–127.

Samadani, R. and Han, C. (1993). Computer-assisted extraction of boundaries from images. In *SPIE: Storage and Retrieval for Image and Video Databases*, pages 219–225.

Serra, J. (1982). *Image Analysis and Mathematical Morphology.* Academic Press, London.

Serra, J., editor (1988). *Image Analysis and Mathematical Morphology. Volume 2: Theoretical Advances.* Academic Press, London.

Stoyan, D., Kendall, W. S., and Mecke, J. (1995). *Stochastic Geometry and its Applications.* Wiley, Chichester, 2nd edition.

Tang, Y. T. and Suen, C. Y. (1993). Image transformation approach to nonlinear shape restoration. *IEEE Transactions on Systems, Man and Cybernetics*, 23:155–171.

Tomita, F. and Tsuji, S. (1977). Extraction of multiple regions by smoothing in selected neighborhoods. *IEEE Transactions on Systems, Man and Cybernetics*, 7:107–109.

van de Vooren, J. G. and van der Heijden, G. W. A. M. (1993). Measuring the size of French beans with image analysis. *Plant Varieties and Seeds*, 6:47–53.

van der Heijden, G. W. A. M., Vossepoel, A. M., and Polder, G. (1996). Measuring onion cultivars with image analysis using inflection points. *Euphytica*, 87:19–31.

Wang, D. C. C., Vagnucci, A. H., and Li, C. C. (1983). Digital image enhancement: a survey. *Computer Vision, Graphics and Image Processing*, 24:363–381.

Wu, H. S. and Barba, J. (1995). An efficient semi-automatic algorithm for cell contour extraction. *Journal of Microscopy*, 179:270–276.

Wu, W., Wang, M. J., and Liu, C. (1992). Performance evaluation of some noise reduction methods. *CVGIP: Graphical Models and Image Processing*, 54:134–146.

Yang, Y. H., Buckley, M. J., Dudoit, S., and Speed, T. P. (2000). Comparison of methods for image analysis on cDNA microarray data. (Available at www.stat.Berkeley.EDU/users/terry/zarray/Html/image.html).

Young, D., Glasbey, C. A., Gray, A. J., and Martin, N. J. (1998). Towards automatic cell identification in DIC microscopy. *Journal of Microscopy*, 192:186–193.

Zahn, C. T. and Roskies, R. Z. (1972). Fourier descriptors for plane closed curves. *IEEE Transactions on Computers*, 21:269–281.